Voltage Dips and Converter-Connected Distributed Generation Units

Bert Renders[1], Lieven Degroote[1], Kurt Stockman[2] and Lieven Vandevelde[1]

[1]Ghent University, Electrical Energy Laboratory (EELAB),
Department of Electrical Energy, Systems and Automation (EESA), Gent, Belgium.
Email: Bert.Renders@UGent.be

[2]Hogeschool West-Vlaanderen, Provinciale Industriële Hogeschool (PIH), Kortrijk, Belgium.

Abstract - The interaction between converter-connected distributed generation units and voltage dips will become increasingly important. This paper focusses on the relation between the behaviour of converters during voltage dips and their current control strategy. A comparison is made between a recently proposed control strategy with programmable damping resistance and the classical sinewave control algorithm. The first-mentioned control structure will prove to yield an improved voltage dip immunity. Experimental tests on a single-phase full-bridge bidirectional converter are carried out and validate the aforementioned postulations. Moreover, the retained voltage at the point of connection of the DG unit will increase thanks to the implementation of the damping control strategy.

1. Introduction

Voltage dips are momentary decreases in rms voltage caused by a short-duration increase in grid current originating from motor starting, transformer energizing or faults in the electric supply system. Voltage dips have been proven to be one of the most important aspects of power quality [1]. Many solutions to mitigate voltage dip related economic damage have been proposed, e.g. the dynamic voltage restorer (DVR), FACTS-devices, series active filters and a wide variation of UPS systems.

The increased presence of grid-connected electronic equipment that is highly sensitive to grid disturbances, emphasizes the necessity to reduce the effects of voltage dips. On the one hand, this can be accomplished by increasing the voltage dip immunity of sensitive equipment such as personal computers [2], AC drives [3,4] and, more generally, voltage source converters [5]. On the other hand, improvement of the support of the utility grid given by grid-connected distributed generation (DG) units proves to be a complementary solution [6]. With most of the solutions to increase voltage dip immunity at the load side, the converter absorbs additional line currents from an already weakened grid. Therefore, the power injected by DG units could make the difference between recovery and instability.

The growing interest in environmental issues, combined with the progress of technologies to couple renewable energy sources to the grid and the liberalization of the energy market have led to a growing share of grid-connected DG. The primary energy sources most often used in these small-scaled applications are wind, solar power, small combined heat and power units, fuel cells and hydro power. In spite of the growing number of DG units, their contribution of power delivered to the utility grid remains small, as compared to the power injected by the large centralized power plants.

2. Current control strategy

In this paper, the behaviour of converter-connected DG-units during voltage dips will be investigated. The behaviour of the converter is strongly dependent on the implementation of its current control loop. Therefore, two different control strategies are compared, and their behaviour during voltage dips is experimentally verified.

The first current controller tries to shape the grid currents as a perfect sinewave, even when the grid voltage is distorted. The amplitude of the sinewave is adapted in order to control the power delivered to the utility grid. This type of current controller can be found in almost all commercial available DG converters [7]. The reference value for the inductor current i_{L}^* is the product of the emulated fundamental conductance g and a sinusoidal reference signal $\sin(\theta_{\text{PLL}})$ generated by a phase-locked loop (PLL):

$$i_{\text{L}}^* = g \sin(\theta_{\text{PLL}}). \tag{1}$$

The second current controller is designed to shape the grid currents in a more complex way. The inductor current is constructed from two parts. The available DG power is transferred into the utility grid using a sinewave with variable

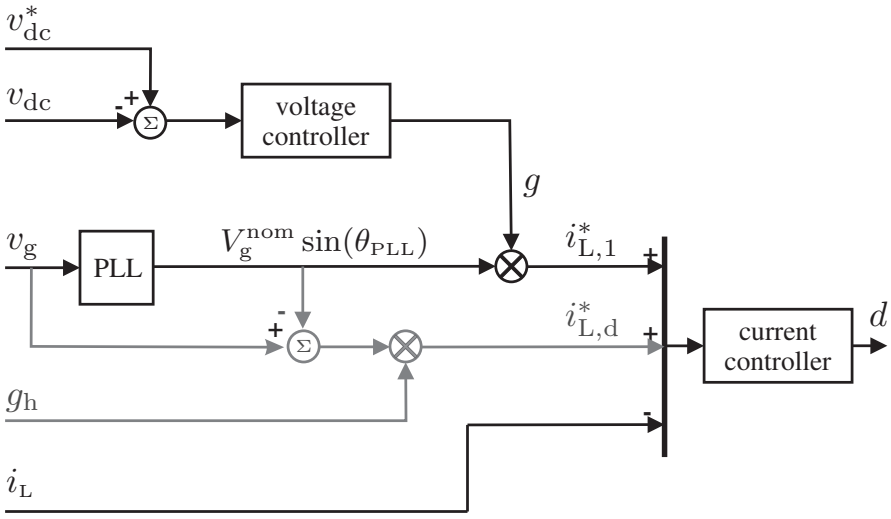

Figure 1: Control strategy for a grid-connected converter with programmable resistive impedance

amplitude, as does the classical current controller. Then, another current waveform is superposed on this sinewave, as can be seen below:

$$i^*_{\text{L}} = g\sin(\theta_{\text{PLL}}) + g_{\text{h}}\left(v_{\text{g}} - \sin(\theta_{\text{PLL}})\right). \tag{2}$$

The second term of the equation is swiftly varying, as it will react on every deviation of the grid voltage v_{g} from its steady-state value. The current originating from voltage disturbances is determined by the programmable damping resistance g_{h}. This control strategy damps grid disturbing phenomena, and was used before to obtain a resistive input impedance for harmonic frequencies [8] in order to damp harmonic oscillations in the utility network [9].

The third commonly used control algorithm, used to obtain purely resistive converters, shapes the inductor current proportional to the grid voltage. However, this algorithm is less suited for grid-connection of distributed generation units, since the converter impedance for harmonics becomes negative when injecting power in the grid. Consequently, this may cause instability. Moreover, the converter behaviour during voltage dips causes premature converter shutdowns. Therefore, the control algorithm is not included in the scope of this paper.

3. Instantaneous response to voltage dips

The instantaneous response of the converter to voltage dips is independent of the bus voltage controller. The bus voltage controller is quite slow, and does not adapt g to a new steady-state value immediately. In other words, for short-time voltage dips the emulated fundamental conductance g can be treated as a constant value.

The grid voltage and the inductor currents of the converter with control strategies as discussed above during a 30% voltage dip are depicted in Fig. 2 as gray and black lines respectively. The power injected in the utility grid is 200 Watt. The plots are made using an experimental setup. The dashed black line represents the grid current of the sinewave converter. The grid current remains unchanged during the voltage dip, as could be expected based on (1). The full black line represents the grid current of the converter with programmable damping resistance. The grid voltage is measured, and the reference value for the grid current is adapted based on these measurements. In Fig. 2, a transient phenomenon can be discerned. Due to the immediate change of the grid voltage v_{g}, an unbalance is created between v_{g} and v_{sw}. Since the current controller is not ideal, the inductor current increases until v_{sw} is adapted by the current controller. This effect can be discerned well in the inductor current of the sinusoidal converter (dashed black line). This effect cannot be noticed in the inductor current of the converter with programmable damping resistance. However, the effect is present but is concealed by the amplitude variation of the inductor current.

The grid voltage v_{g} is supposed to be sinusoidal during the dip, the inductor current i_{L} will thus also be sinusoidal. The magnitude change of the inductor current can be predicted based on (2):

$$\Delta|i_{\text{L}}| = g_{\text{h}}|v_{\text{g}}|D, \tag{3}$$

with D the relative magnitude of the voltage dip and $|v_{\text{g}}|$ and $(1-D)|v_{\text{g}}|$ the magnitude of the grid voltage before and during the voltage dip respectively. Application of this formula on the experimental setup used to create Fig. 2,

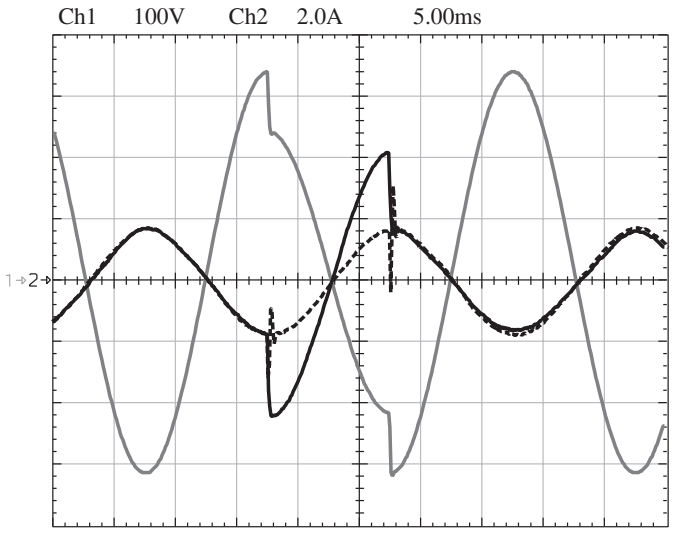

Figure 2: Grid voltage and grid currents during a 30% voltage dip. Gray line: grid voltage, full black line: inductor current of the converter with programmable damping resistance, dashed black line: inductor current of the sinewave converter.

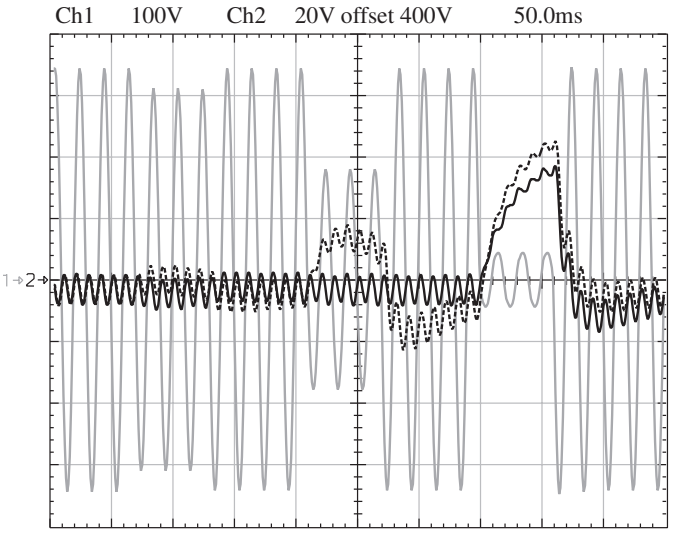

Figure 3: Bus voltage of the converter with programmable damping resistance (full black line) and the sinewave converter (dashed black line) during a series of increasing grid voltage dips (full gray line)

would result in a increase of the inductor current of

$$\Delta|i_{\mathrm{L}}| = \frac{1}{40\Omega} \cdot 325\mathrm{V} \cdot 0.3 = 2.4\mathrm{A}, \tag{4}$$

which matches the waveforms depicted in Fig. 2.

4. Voltage dip ride-through capability

The main reason for converter-connected DG-units to disconnect during voltage dips, is an excessive bus voltage v_{dc}, which causes a trip of the corresponding protection relay and the immediate shutdown of the converter. The bus voltage is dependent of the power injected in the utility grid P_{ac} and the power delivered to the converter by the DG power source P_{dc}.

Based on Fig. 2, the influence of the control strategy on the power injected in the utility grid can be deduced. The sinewave converter undergoing a voltage dip injects less power in the grid compared to the situation before the voltage dip. The resulting power excess at the dc-side of the converter is absorbed in the bus capacitor, resulting in a significant bus voltage rise. The power injected by the converter with programmable damping resistance is not always decreased during the voltage dip. The transmitted power is dependent on the severity of the voltage dip.

To test the voltage dip ride-through capability, the converter is put through a series of dips with increasing dip magnitude. The bus voltage $v_{\mathrm{dc}}(t)$ and the line voltage $v_{\mathrm{g}}(t)$ are depicted in Fig. 3 as full and dashed lines respectively. The experimental results validate the superior voltage ride-through capability of the converter with programmable damping resistance. The sinewave converter can be found to experience higher bus voltages during voltage dips as compared to the converter with programmable damping resistance. An extensive analysis has been made in [10].

5. Increasing the retained voltage

Thanks to the behavior of distributed generation systems during voltage dips, and the resulting change of the power flow through the low voltage distribution feeder, the voltage at the equipment terminals along this feeder will be affected by their presence. In order to quantify the voltage at the equipment terminals, the DG unit is modeled as a voltage source $\overline{E}_{\mathrm{DG}}$ in series with an impedance $\overline{Z}_{\mathrm{DG}}$. This Thévenin equivalent is similar to the one used to investigate the effects of induction motors on voltage dips in [1].

The converter controlled by the damping control strategy, reacts according to (2). The corresponding Thévenin

Table 1: Active and reactive power of the loads in nominal conditions

	POC1	POC2	POC3	POC4	POC5	POC6	POC7	POC8	POC9	POC10
P [KW]	5	7	3	4.5	9	10	3	1	2	5
Q [KVAR]	1	0.5	0.2	3	0	0	1	0	4	2

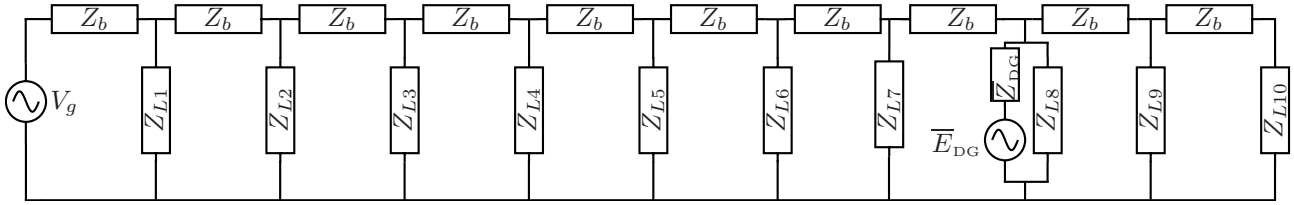

Figure 4: Schematic overview of the distribution feeder

equivalent is given by:

$$\begin{aligned} \overline{Z}_{\mathrm{DG}} &= -\frac{1}{g} \\ \overline{E}_{\mathrm{DG}} &= \frac{g - g_{\mathrm{h}}}{g}(\overline{V}_{\mathrm{g}} - V_{\mathrm{g}}^{\mathrm{nom}} e^{j\theta_{\mathrm{PLL}}}), \end{aligned} \tag{5}$$

keeping in mind that the conductance g is negative when injecting power into the grid. The model allows to investigate the control strategies described above by choosing the value of g_{h}. The parameter g allows to represent the power injected in the grid. The power level of the converter can vary between zero and the nominal power of the DG units, which corresponds with g varying between 0 and -1.

The radial low-voltage distribution feeder studied in this paper is a single-phase residential distribution feeder. A schematic overview of the studied power system is given in Fig. 4. The points of connection (POC) are chosen equidistant. At each of these 10 points of connection, both a residential load and a distributed generator can be connected. The impedance values of the feeder are chosen to obtain a grid impedance at the last point of connection which equals the reference grid impedance [11].

The loads are at first instance chosen to be constant impedance loads, with values as given in Table 1. The choice of these values is arbitrary, and results in a certain voltage profile. This voltage profile is changed due to the connection of DG units. A distributed generator producing 25 kW is connected to POC8.

To analyse the influence of the DG units on the retained voltage during voltage dips a quasi-steady state approach is used. Just before the voltage dip, all loads and DG units are in steady state. At dip initiation, this steady state condition is perturbed. As the time constants of the power balancing processes differ from load to load, the results are dependent on the size and the type of loads present in the power system. By using a quasi-steady state approach, the power balancing processes in the loads and DG units are neglected. This will allow to draw straightforward conclusions from the experiments.

The voltage profile along the distribution feeder in nominal operation conditions is depicted as a full black line in Fig. 5. As the damping control strategy and the sinusoidal control strategy behave indifferently in nominal conditions, only one curve is depicted. A local maximum can be discerned due to the injection of active power in POC8. During a voltage dip the voltage profile is completely different. The lowest voltage magnitude occurs closest to the fault, in this case closest to the MV/LV transformer. An example of the voltage profile during a dip is shown as a dashed line for the damping control strategy and as a dotted line for the sinusoidal control strategy in Fig. 5, where the voltage at the primary side of the MV/LV transformer is equal to 0.7 pu.

As the dashed line lies above the dotted line for all the points of connection, we can conclude that the damping control strategy increases the retained voltage more than the sinusoidal control strategy does.

6. Conclusion

This paper describes the improvement of the voltage dip ride-through capability of a full-bridge bidirectional converter by means of the implementation of an alternative current control strategy. The current control strategy with a

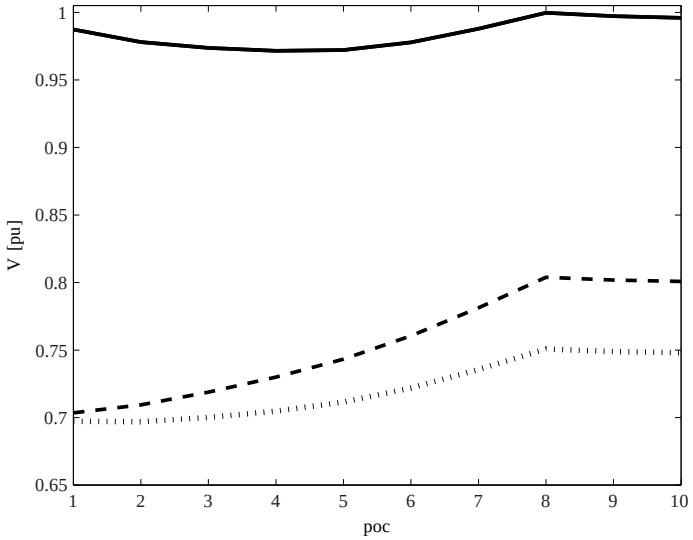

Figure 5: RMS-voltage along the distribution feeder.
full black line: nominal condition, dashed line: damping control strategy during a voltage dip, dotted line: sinusoidal control strategy during voltage dip.

programmable damping resistance has been compared to the classical sinewave control strategy. In both current control strategies the effects of a voltage dip have been analyzed, the response of the converters has been compared and experimentally verified and the effects on the voltage dip ride-through capability have been described. The converter with programmable damping resistance, which was originally designed to provide damping for harmonic oscillations in the utility grid, has showed a significantly better voltage dip immunity. Moreover, the retained voltage along the distribution feeder was also increased more by the damping control strategy than the sinusoidal control strategy. Implementing the damping control strategy thus benefits the DG unit as well as the grid.

References

[1] M. H. J. Bollen, *Understanding power quality problems*, ser. Power Engineering. IEEE press, 2000.

[2] S. Djokić, J. Desmet, G. Vanalme, J. V. Milanović, and K. Stockman, "Sensitivity of personal computers to voltage sags an short interruptions," *IEEE Trans. Power Delivery*, vol. 20, no. 1, pp. 375–383, Jan. 2005.

[3] K. Stockman, F. D'hulster, K. Verhaege, J. Desmet, and R. Belmans, "Voltage dip immunity test set-up for induction motor drives," in *Proc. 11th Int. Symp. Power Electron.*, Novi Sad, Yugoslavia, Oct.31-Nov.2 2001.

[4] M. H. J. Bollen and L. D. Zhang, "Analysis of voltage tolerance of AC adjustable-speed drives for three-phase balanced and unbalanced sags," *IEEE Trans. Ind. Applicat.*, vol. 36, no. 3, pp. 904–910, May/June 2000.

[5] A. Sannino, M. H. J. Bollen, and J. Svensson, "Voltage tolerance testing of three-phase voltage source converters," *IEEE Trans. Power Delivery*, vol. 20, no. 2, pp. 1633–1639, Apr. 2005.

[6] K. J. P. Macken, M. H. J. Bollen, and R. J. M. Belmans, "Mitigation of voltage dips through distributed generation systems," *IEEE Trans. Ind. Applicat.*, vol. 40, no. 6, pp. 1686–1693, Nov./Dec. 2004.

[7] S. B. Kjaer, J. K. Pedersen, and F. Blaabjerg, "A review of single-phase grid-connected inverters for photovoltaic modules," *IEEE Trans. Ind. Applicat.*, vol. 41, no. 5, pp. 1292–1306, Sept./Oct. 2005.

[8] B. Renders, K. De Gussemé, W. R. Ryckaert, and L. Vandevelde, "Input impedance of grid-connected converters with programmable harmonic resistance," *IET Electr. Power Appl.*, vol. 1, no. 3, pp. 355–361, May 2007.

[9] W. R. Ryckaert, K. De Gussemé, D. M. Van de Sype, L. Vandevelde, and J. A. Melkebeek, "Damping potential of single-phase bidirectional rectifiers with resistive harmonic behaviour," *IEE Proc. Electr. Power Appl.*, vol. 153, no. 1, pp. 68–74, Jan. 2006.

[10] B. Renders, W. R. Ryckaert, K. De Gussemé, K. Stockman, and L. Vandevelde, "Improving the voltage dip immunity of converter-connected distributed generation units," *Renew. Energy*, vol. 33, no. 5, pp. 1011–1018, May 2008.

[11] *Considerations on Reference Impedances for Use in Determining the Disturbance Characteristics of Household Appliances and Similar Electrical Equipment*, IEC Std. 60 725, 1981.